ELSEVIER

Soil Dynamics and Earthquake Engineering 28 (2008) 1–6

SOIL DYNAMICS AND EARTHQUAKE ENGINEERING

www.elsevier.com/locate/soildyn

Energy of strong motion at earthquake source

M.D. Trifunac

Department of Civil Engineering, University of Southern California, Los Angeles, CA 90089, USA

Received 4 March 2006; accepted 12 June 2007

Abstract

This note is the first in a series devoted to a study of the flow of earthquake energy from the source to its destination, the soil–structure systems, where it will drive the relative structural response. The basic seismological aspects of empirical scaling of seismic wave energy, E_s, are reviewed, and it is shown how this energy can be represented by functionals of strong ground motion. This constitutes the first required step, after which this energy will be attenuated (dissipated) along the wave propagation path, arriving as the incident-wave energy upon the soil–structure systems. The ultimate goal of this work is to form a basis for formulation of a new design method in which the power of the incident-wave pulses will be compared with the capacity of the structure to absorb this power.

Keywords: Strong motion; Earthquake energy; Source energy

1. Introduction

The classical method of response spectrum superposition [1,2] continues to be a practical tool for design of structures expected to vibrate without any damage during the largest possible levels of shaking. However, pragmatic considerations, analyses of uncertainties, and minimization of cost result in designs of structures that may experience damage from rare and very strong earthquake shaking. Therefore, during the last 30 years many modifications and "corrections" have been introduced into the response spectrum method to reconcile its *linear* nature with its desired *nonlinear* use in design (e.g. [3,4]).

This paper explores an alternative to the spectral method in earthquake-resistant design, by analyzing the flow of energy associated with strong motion. This requires consideration of all of the principal stages of earthquake energy flow, from the earthquake source, along the propagation path, and to the final work leading to relative response of the structure. The loss of energy along the propagation path also has to be considered. These losses must be accounted for to properly quantify the remaining energy, which will excite the relative response of the structures. In this (Paper I), the first in a series, we will analyze only the strong-motion estimates of earthquake energy release at the source.

Well-designed structures are expected to be *ductile* during the largest credible shaking and to have a large energy reserve to at least delay failure if it cannot be avoided. As a structure finally enters large nonlinear levels of response, it absorbs the excess of the input energy through ductile deformation of its components. Thus, it is logical to formulate earthquake-resistant design procedures in terms of the energy driving this process [5,6]. From the mechanics point of view, this involves nothing new, since the basic energy equations can be derived directly from Newton's second law. The advantage of using energy is that the duration of strong motion, the number of cycles to failure, and dynamic instability, all can be considered directly and explicitly. This, of course, requires scaling of the earthquake source and of the attenuation of strong motion to be described in terms of energy.

Ideas to use energy in seismic design can be traced back to the 1930s, when Benioff [7] proposed the use of seismic destructiveness, to be measured by computing the area under the relative displacement response spectrum. It can be shown that this result can be related to the energy of strong motion [8,9].

The seismological and earthquake engineering characterizations of the earthquake source begin with the

E-mail address: trifuna@usc.edu

0267-7261/$ - see front matter © 2007 Elsevier Ltd. All rights reserved.
doi:10.1016/j.soildyn.2007.06.009

estimation of its "size." For centuries this was done in terms of earthquake intensity scales, which are not instrumental and are based on human description of the effects of earthquakes [10,11]. In the early 1930s, the first instrumental scale—the local earthquake magnitude, M_L—was introduced in southern California [10,12]. Few years later, it was followed by the surface-wave magnitude, M_s [13,14], and more recently by the moment magnitude, $M_w = (\log_{10} M_0 — 16)/1.5$, and by the strong-motion magnitude, M_L^{SM} [15]. The seismic energy associated with elastic waves radiated from the source, E_s, [13,14] has also been used to compare "sizes" of different earthquakes. The seismic energy, E_s, leaving the earthquake source is attenuated with increasing epicentral distance, r, through mechanisms of inelastic attenuation [16], scattering, and geometric spreading. In the near field, for distances comparable to the source dimensions, different near-field terms attenuate like r^{-4} and r^{-2} [17]. The body waves (P- and S-waves) attenuate like r^{-1}, while the surface waves attenuate like $r^{-1/2}$.

The seismic wave energy arriving at the site is next attenuated by the nonlinear response of shallow sediments and soil in the "free field" [18–21] before it begins to excite the foundation. Once the foundation is excited by the incident waves, the response of the soil–structure system is initiated. The incident-wave energy is further reduced by the nonlinear response of the soil during soil–structure interaction [22–25] and by radiation damping [26,27]. The seismic energy flow and distribution during the final three stages—(1) the response of the soil-foundation–structure systems, (2) the energy available to excite the structure, and (3) the relative response of the structure—will be analyzed in future papers.

2. Earthquake source energy

During an earthquake, the potential energy in the rocks is converted into heat, into mechanical work moving the crustal blocks and crushing the material in the fault zone, and into energy, E_s, associated with the emitted elastic waves. At a given period, the energy in the elastic waves is of the form

$$\log_{10} E_s = C + 2M, \tag{1}$$

where C is a constant and M is the earthquake magnitude. Following numerous estimates of the energy radiated by different earthquakes and revisions of the empirical scaling equations based on Eq (1) using surface-wave magnitude, M_s, this empirical relationship has evolved to become [14]

$$\log_{10} E_s = 4.8 + 1.5\, M_s(\text{Jouls}). \tag{2}$$

In terms of the local magnitude scale M_L, this is equivalent to [10]

$$\log_{10} E_s = 9.9 + 1.9\, M_L - 0.024\, M_L^2\ (\text{ergs}) \tag{3a}$$

or

$$\log_{10} E_s = 2.9 + 1.9\, M_L - 0.024\, M_L^2\ (\text{Jouls}). \tag{3b}$$

For scaling in terms of earthquake intensity scales, we mention the work of Shebalin [28], who proposed the following empirical relationship:

$$0.9 \log_{10} E_s - I = 3.8 \log_{10} h - 3.3, \quad \text{for} \quad h < 70\,\text{km}, \tag{4}$$

where E_s is the energy in surface waves in MJouls (10^{13} ergs), h is hypocentral depth in kilometers, and I is the maximum modified Mercalli intensity.

The amount of energy transmitted per unit of time, across unit area, normal to the direction of wave propagation, is $\rho\alpha v^2$ for plane P-waves and $\rho\beta v^2$ for plane S-waves, where ρ is material density, α is velocity of P-waves, β is velocity of S-waves, and v is particle velocity. The shear-wave energy transmitted through area A during time interval $[0, T]$ is, for example,

$$E_s = \rho A \beta \int_0^T v^2(t)\, \mathrm{d}t, \tag{5}$$

with analogous expression for the energy of P-waves. Using Parceval's theorem, Eq. (5) becomes

$$E_s = \frac{\rho A \beta}{2\pi} \int_0^\infty \left(\frac{F(\omega)}{\omega} \right)^2 \mathrm{d}\omega, \tag{6}$$

where $F(\omega)$ is the Fourier amplitude spectrum of ground acceleration (Fig. 1). For practical calculations using band-limited strong-motion data, Trifunac [31] defined the quantity en (proportional to energy) as

$$en = \int_{\pi/50}^{200\pi} \left| \frac{F(\omega)}{\omega} \right|^2 \mathrm{d}\omega. \tag{7}$$

To account for all of the radiated energy in the form of elastic waves, and to follow its attenuation and distribution, starting with the earthquake source and ending with the structural response, it is first necessary to show that the above simple expressions, valid only for plane waves, can be used to approximately account for all of the elastic energy, E_s, radiated by the source. As a first step, we show that E_s computed from Eq (6), where $F(\omega)$ is determined from empirical scaling equations for Fourier amplitude spectra of recorded strong-motion accelerograms [16,32], is approximately equal to E_s in Eq (2), based on seismological estimates of Local, M_L , and surface (M_s) wave magnitudes. In Fig. 2, we plot $\log_{10}(2\rho_{source}\beta_{source}A_{source}en)$ versus $\log_{10} E_s$, computed from Eqs (2) and (3b), for $M = 4$, 5, 6, 7, and 8. For this example, we take $\beta_{source} = 3\,\text{km/s}$, $\rho_{source} = 2 \times 10^3\,\text{kg/m}^3$ and source area $A_{source} = LW$, where L and W are the fault length and width, given by [16,32]:

$$L = 0.01 \times 10^{0.5M}(\text{km}), \tag{8}$$

and

$$W = 0.1 \times 10^{0.25M}(\text{km}). \tag{9}$$

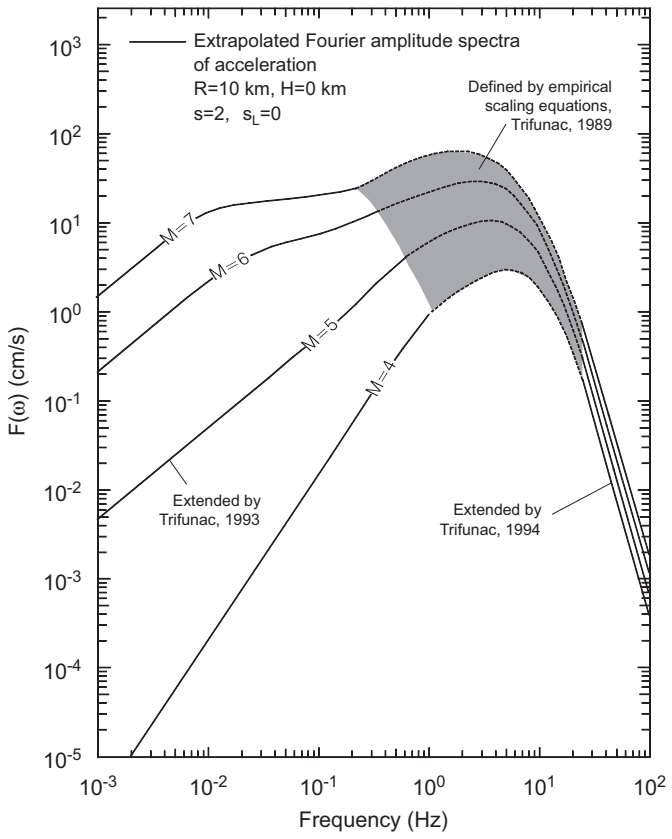

Fig. 1. Fourier amplitude spectra of ground acceleration at a site on geological basement rock ($s = 2$; see [29]) and "rock" soil ($s_L = 0$), for earthquake magnitudes $M = 4,5,6,$ and 7, zero source depth and epicentral distance $R = 10$ km. The shaded region indicates the range in which the empirical scaling laws apply [30].

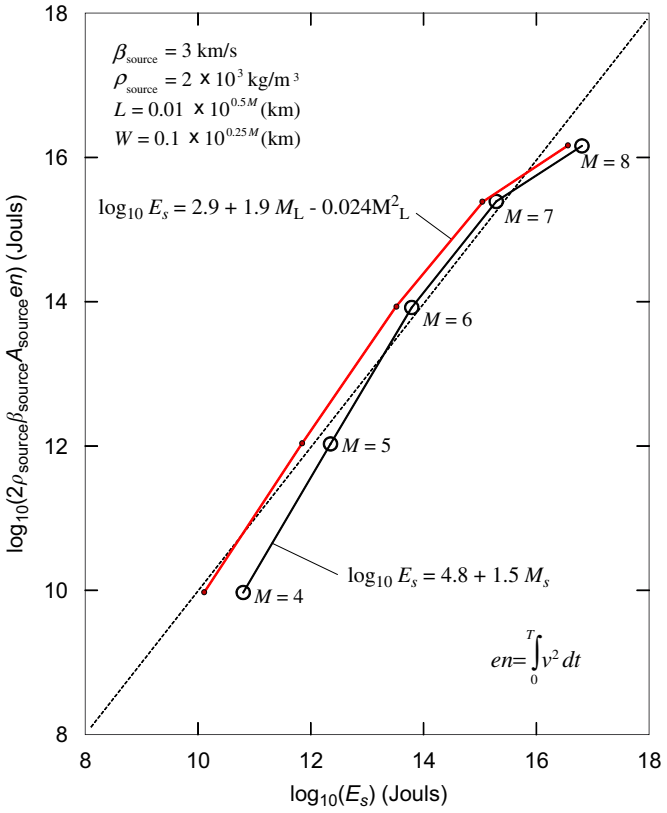

Fig. 2. Energy computed from empirical equations describing recorded strong-motion velocity, extrapolated to the fault surface, ($2p_{\text{source}}\beta_{\text{source}}$ A_{source} en), versus seismological (empirical) definition of E_s in terms of earthquake magnitude.

It can be seen that $2\rho_{\text{source}}\beta_{\text{source}}A_{\text{source}} \sim E_s$. The factor of 2 comes from the fact that we approximated the area through which E_s is radiated by $2A$, representing both sides of the fault plane. The agreement found in Fig. 2 implies that our empirical scaling equations for $F(\omega)$ [16,30,32], including their extrapolation to the fault surface, are satisfactory and that they can be used for strong-motion estimates of radiated energy.

3. An example with recorded data

The following example shows how the energy in recorded strong-ground motion can be used to compute the magnitude of an earthquake, and thus to test the above scaling. We present this example for the Northridge, California, and earthquake of January 17, 1994.

Fig. 3 shows the horizontal projection of the fault plane (dashed lines). The gray shades in this figure outline the areas where the basement rock is essentially at the surface. To minimize the effects of amplification by sediments and thus simulate conditions of typical seismological observatories, we consider only those sites of strong-motion stations that recorded this event on basement rock. This requirement led to the selection of 25 strong-motion stations, as shown in Fig. 3. At each of these stations, we compute $\int_0^T v^2(t)\,\mathrm{d}t$ for the entire duration of all available recorded components and assume that the result is an approximation of *en* in Eq. (7). We combine contribution from three components of motion by square root of the sum of the squares. To correct for average inelastic attenuation and geometric spreading, we multiply all of the recorded velocities by $\Delta \exp(\omega\Delta/2Q\beta)$, where Δ is hypocentral distance and Q is the quality factor. We assume $\omega \sim 6.28$ rad/s, $\beta \sim 1$ km/s, and $Q = 500$. Finally, we multiply the integrals of velocities squared by $\rho_{\text{source}} \cdot \beta_{\text{source}} \cdot A_{\text{source}}$ and assume that $\rho_{\text{source}} = 1.6 \times 10^3\ \text{kg/m}^3$, $\beta_{\text{source}} = 1$ km/s, and $A_{\text{source}} = 100\ \text{km}^2$ [33]. From the computed E_s (using Eq (5)), we evaluate M_s using Eq. (2). The results are shown in Fig. 4. The data indicates an average estimate equal to $M_s = 6.7$ and a standard deviation of 0.20. This is in good agreement with other magnitude estimates for the Northridge earthquake (local magnitude $M_L = 6.4$ and moment magnitude $M_w = 6.7$ [33].

Other examples of using wave energy to interpret recorded strong-motion accelerations can be found in Trifunac [34, 35].

The nature of growth of the integral in Eq. (5) versus time is shown in Fig. 5. It increases rapidly at first, and then tends asymptotically toward its final value. The time during which this integral grows rapidly is called the

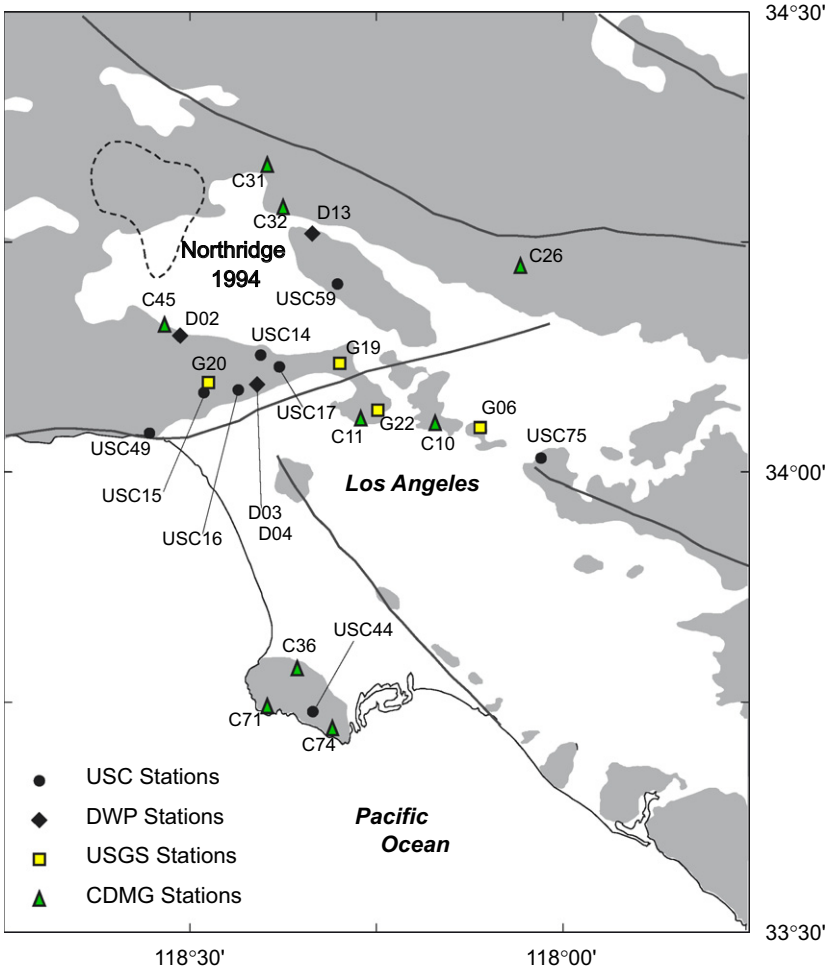

Fig. 3. Twenty-five strong-motion stations on basement rock, during Northridge, California earthquake of January 1994.

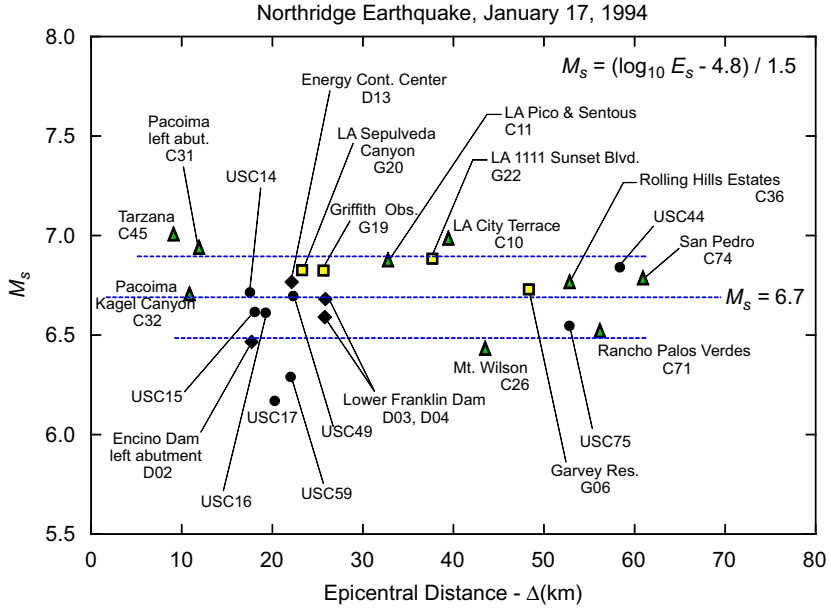

Fig. 4. Surface-wave magnitude, M_s, computed from E_s (corrected for geometric spreading and anelastic attenuation), versus epicentral distance. All points shown are for stations located on basement rock (see Fig. 3).

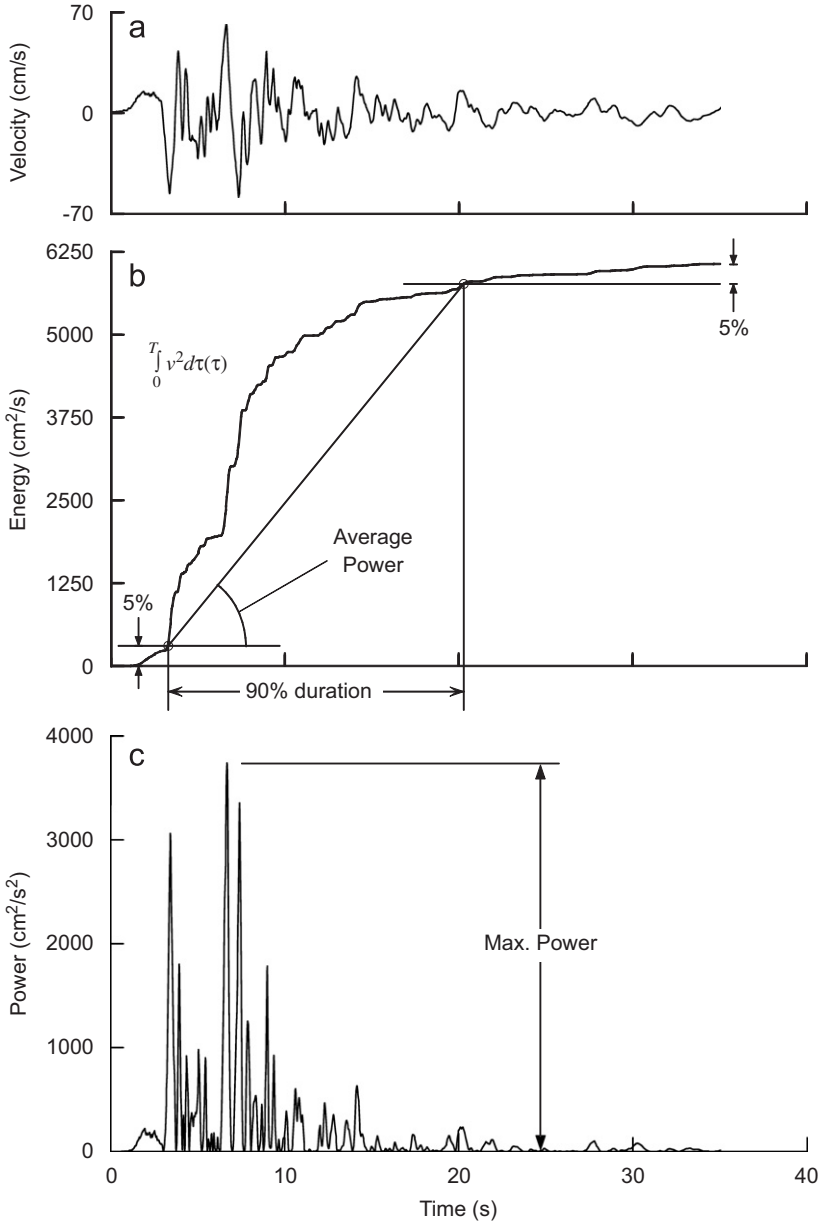

Fig. 5. Strong-motion velocity (top), "wave energy" $\left(\int_o^t v^2(t)\,\mathrm{d}t\right)$ and its (90 percent) duration (center), and maximum incident power $\left(\frac{\partial}{\partial t}\int_o^t v^2(t)\,\mathrm{d}t\right)$ (bottom).

"strong-motion duration," and in this example it corresponds to realization of 90 percent of strong-motion energy at this site. The duration of the strong-motion increases with magnitude, epicentral distance, depth, and dimensions of sedimentary layers through which the waves propagate (e.g., see the review article by [36]). Fig. 5 (bottom) shows the power of strong motion, computed by differentiation of *en* (center), with respect to time. Maximum power and the duration will be of particular interest in estimation of the maximum seismic demand on structures [5].

4. Conclusions

It has been shown how the radiated strong-motion energy leaving the earthquake source can be approximated, using Parceval's Theorem, in terms of the integrals of Fourier amplitude spectra of strong-motion acceleration. The accuracy of this approach was illustrated by an example from the Northridge, California, and earthquake of 1994. It was then shown how the magnitude of an earthquake could be estimated (with standard deviation of about 0.2), by using the energy integrals of the spectral amplitudes of strong motion. From this experiment we conclude that Eq. (6) can be used to estimate seismic wave energy E_s, radiated by a fault.

The scaling Eq. (6) for E_s provides a starting point for the studies of attenuation of the seismic wave energy with distance from the earthquake source, and for scaling of the total energy demand, and of the associated power demand, of the waves arriving towards the building site.

References

[1] Biot MA. A mechanical analyzer for the prediction of earthquake stresses. Bull Seism Soc Am 1941;31(2):151–71.

[2] Biot MA. Analytical and experimental methods in engineering seismology. ASCE Trans 1942;108:365–408.

[3] Jalali RS, Trifunac MD, Ghodrati AG, Zahedi M. Wave-passage effects on strength-reduction factors for design of structures near earthquake faults. Soil Dyn Earthquake Eng 2007;27(8): 703–11.

[4] Jalali RS, Trifunac MD. Strength-reduction factors for structures subjected to differential near-source ground motion. Ind Soc Earthquake Technol J 2007;44(1):287–305.

[5] Trifunac MD. Power design method. In: Proceedings of earthquake engineering in the 21st century to mark 40th anniversary of IZIIS-Skopje, key note lecture, 28 August–1 September 2005, Macedonia: Skopje and Ohrid, 2005.

[6] Gicev V, Trifunac MD. Energy and power of nonlinear waves in a seven story reinforced concrete building. Ind Soc Earthquake Technol J 2007;44(1):307–25.

[7] Benioff H. The physical evaluation of seismic destructiveness. Bull Seism Soc Am 1934;24:398–403.

[8] Arias A. A measure of earthquake intensity, in seismic design of nuclear power plants. Hansen RJ., editor. The Mass Inst of Tech Press, 1970.

[9] Trifunac MD, Brady AG. A study of the duration of strong earthquake ground motion. Bull Seism Soc Am 1975;65:581–626.

[10] Richter CF. Elementary seismology. San Francisco: Freeman and Co; 1958.

[11] Trifunac MD, Brady AG. On the correlation of seismic intensity scales with the peaks of recorded strong ground motion. Bull Seism Soc Am 1975;65:139–62.

[12] Richter CF. An instrumental earthquake magnitude scale. Bull Seism Soc Am 1936;25:1–32.

[13] Gutenberg B, Richter CF. Earthquake magnitude, intensity, energy, and acceleration. Bull Seism Soc Am 1956;46(2):105–45.

[14] Gutenberg B, Richter CF. Magnitude and energy of earthquakes. Ann Geofisica 1956;9:1–15.

[15] Trifunac MD. M_L^{SM}. Soil Dyn Earthquake Eng. 1991;10(1):17–25.

[16] Trifunac MD. Q and high-frequency strong-motion spectra. Soil Dyn Earthquake Eng. 1994;13(3):149–61.

[17] Haskell NA. Elastic displacements in the near field of a propagating fault. Bull Seism Soc Am 1969;59:865–908.

[18] Joyner WB. A method for calculating nonlinear seismic response in two dimensions. Bull Seism Soc Am 1975;65(5):1337–57.

[19] Joyner WB, Chen ATF. Calculating of nonlinear ground response in earthquakes. Bull Seism Soc Am 1975;65(5):1315–36.

[20] Trifunac MD, Todorovska MI. Nonlinear soil response–1994 Northridge California, earthquake. J Geotechnical Eng ASCE 1996; 122(9):725–35.

[21] Trifunac MD, Todorovska MI. Nonlinear soil response as a natural passive isolation mechanism—the 1994 Northridge, California earthquake. Soil Dyn Earthquake Eng 1998;17(1):41–51.

[22] Gicev V. Investigation of soil-flexible foundation-structure interaction for incident plane SH waves. Ph.D. dissertation, Department of Civil Engineering, University of Southern California, Los Angeles, California, 2005.

[23] Trifunac MD, Ivanović SS, Todorovska MI, Novikova EI, Gladkov AA. Experimental evidence for flexibility of a building foundation supported by concrete friction piles. Soil Dyn Earthquake Eng 1999; 18(3):169–87.

[24] Trifunac MD, Ivanović SS, . Todorovska MI. Apparent periods of a building, Part I: Fourier analysis. J Struct Eng ASCE 2001; 127(5):517–26.

[25] Trifunac MD, Ivanović SS, Todorovska MI. Apparent periods of a building, Part II: time-frequency analysis. J Struct Eng ASCE 2001; 127(5):527–37.

[26] Luco JE, Trifunac MD, Wong HL. Soil–structure interaction effects on forced vibration tests. Department of Civil Engineering Report no. 86–05, University of Southern California, Los Angeles, California, 1985.

[27] Todorovska MI, Trifunac MD. Radiation damping during two-dimensional building soil interaction. Department of Civil Engineering, Report no. 91-01, Universityof Southern California, Los Angeles, CA, 1991.

[28] Shebalin NV. O svyazi mezhdu energey, balnostyu i glubinoy ochaga zemletryaseniya. Izvestiya Akad. Nauk SSSR, Ser Geofiz, 1955. 377–80.

[29] Trifunac MD. How to model amplification of strong earthquake motions by local soil and geologic site conditions. Int J Earthquake Eng Struct Dyn 1990;19(6):833–46.

[30] Trifunac MD. Dependence of Fourier spectrum amplitudes of recorded strong earthquake accelerations on magnitude, local soil conditions and on depth of sediments. Earthquake Eng Struct Dyn 1989;18(7):999–1016.

[31] Trifunac MD. Empirical criteria for liquefaction in sands via standard penetration tests and seismic wave energy. Soil Dyn Earthquake Eng 1995;13(3):149–61.

[32] Trifunac MD. Long period Fourier amplitude spectra of strong motion acceleration. Soil Dyn Earthquake Eng 1993;12(6):363–82.

[33] Wald DJ, Heaton TH, Hudnut KW. The slip history of the 1994 Northridge, California, earthquake determined from strong-motion, Telseismic, GPS, and leveling data. Bull Seism Soc Am 1996; 86(1B):S49–70.

[34] Trifunac MD. Stress estimates for San Fernando, California earthquake of February 9, 1971: main event and thirteen aftershocks. Bull Seism Soc Am 1972;62:721–50.

[35] Trifunac MD. Tectonic stress and source mechanism of the Imperial Valley, California earthquake of 1940. Bull Seism Soc Am 1972; 62:1283–302.

[36] Trifunac MD, Novikova EI. State-of-the-art review on strong-motion duration. 10th Eur Conf Earthquake Eng 1994;I:131–40.